

Uniform relativistic motion through a thermal bath as a thermodynamic resource

Rahul Shastri^{1,*}

¹*Department of Optics, Palacky University, 17. listopadu 1192/12, 779 00 Olomouc, Czech Republic*

We show that a quantum system undergoing motion with uniform relativistic velocity through a thermal bath consisting of a massless scalar field is generically driven into a non-equilibrium steady-state (NESS) solely due to its motion, even in the absence of external driving or multiple baths. The relative motion between the system and the bath breaks detailed balance, preventing thermalization to a Gibbs state. We find that the resulting steady-states fall into two distinct classes: (i) NESSs with persistent probability currents, and (ii) current-free non-Gibbs steady states characterized by a frequency-dependent effective inverse temperature. We demonstrate, using a three-level system, that NESSs with probability current can function as noisy stochastic clock, while current-free non-Gibbs steady states possess non-zero non-equilibrium free energy, indicating their potential as a quantum battery for work extraction or storage.

Introduction—One of the central aims in the field of quantum thermodynamics is to identify resources that enable tasks beyond those achievable at thermal equilibrium. A system coupled to a single thermal bath at finite temperature is completely passive and cannot perform useful thermodynamic tasks. Consequently, any thermodynamically nontrivial operation requires access to resources beyond a single equilibrium bath. It is now well established that nonequilibrium resources such as coherence [1], entanglement and correlations [2], squeezed reservoirs [3–5], and multiple thermal baths [6] can enable such tasks, underpinning applications in quantum heat engines, quantum batteries, and quantum clocks [7–9].

Independently, a separate research field—relativistic quantum information (RQI)—has emerged to study how relativistic effects and spacetime structure influence quantum systems from a quantum-information theoretic perspective. A central goal of this field is to understand how these effects may be harnessed for quantum information processing tasks. In this context, relativistic motion has been shown to enable entanglement and correlation harvesting [10], magic harvesting [11], etc. Only recently have relativistic effects begun to be explored in thermodynamic settings, including quantum heat engines [12–19], quantum batteries [20, 21], and quantum metrology [22–26]. From the perspective of quantum thermodynamics, this raises a natural question, whether relativistic effects such as relativistic motion or spacetime structure, themselves be regarded as thermodynamic resources?

In standard open quantum system dynamics, a system weakly coupled to a thermal bath relaxes to a thermal state at the bath temperature as a consequence of the Kubo–Martin–Schwinger (KMS) condition satisfied by the bath correlation functions. This condition implies detailed balance between excitation and relaxation rates and guarantees thermalization to a Gibbs state. However, in a relativistic setting where the system follows an arbitrary timelike trajectory with respect to the bath, the correlation function evaluated along the trajectory generally fails to satisfy the standard KMS relation [27–33]. A particularly important case is that of stationary trajectories,

for which the correlation function depends only on the proper-time difference. In this case, the KMS condition is modified and the resulting excitation and relaxation rates satisfy a generalized detailed-balance relation with a frequency-dependent effective inverse temperature. As a result, the steady state reached in the weak-coupling limit is no longer guaranteed to be of Gibbs form. In vacuum (i.e., for a zero-temperature field), stationary trajectories were classified by Letaw and include inertial motion, uniform acceleration, and circular motion, among more exotic cases [27, 32, 34]. At finite temperature, however, this symmetry is reduced and only inertial and uniformly rotating trajectories remain stationary.

In this work, we focus on the simplest stationary trajectory, namely a quantum system undergoing uniform relativistic motion with respect to a thermal bath of a massless scalar field. The quantum system, often referred to as a detector in the RQI literature, is modeled as point-like with no spatial structure. We analyze the resulting steady state in the weak-coupling limit and assess its potential role as a thermodynamic resource. We show that uniform relativistic motion generically drives the system into a non-Gibbs steady state, even in the presence of a single thermal bath. Two distinct classes of steady states emerge: (i) NESSs with persistent probability currents, and (ii) current-free non-Gibbs steady states characterized by a frequency-dependent effective inverse temperature. Using a three-level system as an illustrative example, we demonstrate that the former can function as noisy stochastic clocks, while the latter possess finite nonequilibrium free energy, enabling work extraction or storage from a single thermal reservoir and highlighting their potential as quantum batteries.

Set-up—We consider a point-like non-relativistic quantum system following a time-like trajectory $X(\tau)$, interacting with a bath consisting of a massless quantum scalar field with total Hamiltonian $\hat{H} = \hat{H}_S + \hat{H}_B + \hat{V}$. Here $\hat{H}_S = \sum_{i=0}^{\infty} \epsilon_i |\epsilon_i\rangle \langle \epsilon_i|$ and $\hat{H}_B = \frac{1}{2} \int d^3x \left(\hat{\pi}^2 + (\nabla \hat{\Phi})^2 \right)$ are the Hamiltonians of system and field respectively. Here $\hat{\Phi}(X)$ is the field operator, $\hat{\pi}(X)$ is the conjugate

momentum operator of the field, ϵ_i are energy eigenvalues of the system with corresponding energy eigenstates $|\epsilon_i\rangle$. We consider Unruh-Dewitt interaction $\hat{V}^I(\tau) = \lambda \hat{A}^I(\tau) \otimes \hat{\Phi}(X(\tau))$, where λ is the interaction strength, $\hat{A}^I(\tau) = e^{i\hat{H}_S\tau} \hat{A} e^{-i\hat{H}_S\tau}$ is the system operator in interaction picture and $\hat{\Phi}(X(\tau))$ is field operator evaluated on the trajectory of the system. Starting from factorized initial state and under Born-Markov and secular approximation, we get the Gorini-Kossakowski-Sudarshan-Lindblad (GKSL) master equation for the system (see [35]),

$$\begin{aligned} \frac{\partial \hat{\rho}}{\partial \tau} = & -i [\hat{H}_S + \hat{H}_{LS}, \hat{\rho}] + \sum_{\omega > 0} \Gamma(\omega) \mathcal{D}[\hat{A}_\omega] \hat{\rho} \\ & + \sum_{\omega > 0} \Gamma(-\omega) \mathcal{D}[\hat{A}_\omega^\dagger] \hat{\rho}, \end{aligned} \quad (1)$$

where $\hat{H}_{LS} = \sum_{\omega} \Delta(\omega) \hat{A}_\omega^\dagger \hat{A}_\omega$ is the unitary Lamb-shift term, $\mathcal{D}[\hat{O}] \hat{\rho} = \hat{O} \hat{\rho} \hat{O}^\dagger - \frac{1}{2} \{ \hat{O}^\dagger \hat{O}, \hat{\rho} \}$ is dissipator with anti-commutation operation $\{ \hat{A}, \hat{B} \} = \hat{A} \hat{B} + \hat{B} \hat{A}$ and $\hat{A}_\omega = \sum_{p,k,\omega=\epsilon_p-\epsilon_k} \langle \epsilon_k | \hat{A} | \epsilon_p \rangle | \epsilon_k \rangle \langle \epsilon_p |$ is system operator decomposed in terms of the Bohr frequencies ω , satisfying $[\hat{H}_S, \hat{A}_\omega] = -\omega \hat{A}_\omega$, $[\hat{H}_S, \hat{A}_\omega^\dagger] = \omega \hat{A}_\omega^\dagger$ and $[\hat{H}_S, \hat{A}_\omega \hat{A}_\omega^\dagger] = [\hat{H}_S, \hat{A}_\omega^\dagger \hat{A}_\omega] = 0$ and $\Gamma(\omega)$ is bath spectral function.

We consider the bath to be in stationary thermal Gibbs state at inverse temperature $\beta = 1/T$ with the bath spectral function $\Gamma(\omega) = \lambda^2 \int_{-\infty}^{\infty} d\tau e^{i\omega\tau} G^\beta[X(\tau), X(0)]$, where $G^\beta[X(\tau), X(0)]$ is the Wightman function of the thermal state of the field evaluated along the stationary trajectory $X(\tau)$ of the system (see [35]). In general, for any stationary trajectory and stationary quantum field state, the Wightman function evaluated on the trajectory, satisfies a generalized detailed balance relation of the form,

$$\frac{\Gamma(\omega; \alpha_i)}{\Gamma(-\omega; \alpha_i)} = e^{\beta_{\text{eff}}(\omega; \alpha_i) \omega}, \quad (2)$$

where $\beta_{\text{eff}}(\omega; \alpha_i)$ is frequency-dependent effective inverse temperature and α_i are additional parameters (for example, velocity, acceleration, radius of trajectory, etc) depending on the choice of the stationary trajectory. Here, we focus on a system undergoing motion with uniform velocity along the trajectory $X(\tau)$ given by $X(\tau) = \left(\frac{1}{\sqrt{1-u^2}}, \frac{u}{\sqrt{1-u^2}}, 0, 0 \right) \tau$, where $0 \leq u \leq 1$ is velocity in the units of speed of light c . In this case, the bath spectral function reads (see [35]),

$$\Gamma(\omega; \beta, u) = \begin{cases} \gamma(\omega) [N(\omega, \beta, u) + 1] & \omega > 0 \\ \gamma(|\omega|) N(|\omega|, \beta, u) & \omega < 0, \end{cases} \quad (3)$$

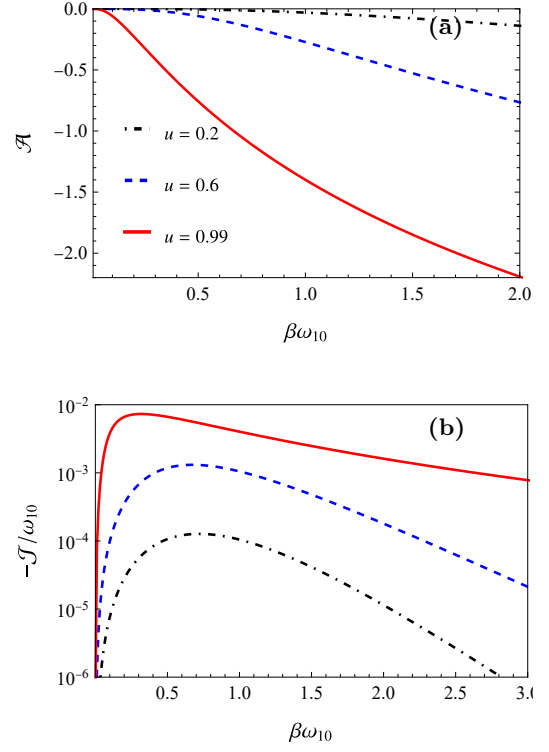


FIG. 1. (Color Online) Affinity \mathcal{A} (a) and current $-\mathcal{J}$ (b) of three level system, as function of inverse temperature β for three different value of velocity small $u = 0.2$ (black dot-dashed), intermediate $u = 0.6$ (blue dashed) and ultrarelativistic $u = 0.99$ (red solid). Other parameter values are $\omega_{10} = 1.0, \omega_{21} = 3.1$.

where

$$\gamma(\omega) = \frac{\lambda^2}{2\pi} \omega \quad (4)$$

$$N(\omega, \beta, u) = \frac{\sqrt{1-u^2}}{2\beta\omega u} \ln \frac{1 - e^{-\beta\omega\sqrt{\frac{1+u}{1-u}}}}{1 - e^{-\beta\omega\sqrt{\frac{1-u}{1+u}}}}. \quad (5)$$

Results– We first look at the steady-state reached by the system in the long time limit following the dynamical equation Eq. (1). Note that the form of Eq. (1) is that of the standard GKLS master equation for thermalisation but with effective occupation number $N(\omega, \beta, u)$ that explicitly depends on velocity u (see [35]). It can be shown that the energy state coherence (i.e. the off-diagonal terms $\rho_{ij} = \langle \epsilon_i | \hat{\rho} | \epsilon_j \rangle$ where $i \neq j$) decay to zero in the long time limit (see [35]). Let us focus on the population dynamics (i.e. the diagonal terms $p_i = \langle \epsilon_i | \hat{\rho} | \epsilon_i \rangle$), which obey the Pauli master equation,

$$\dot{p}_i = - \sum_j J_{i \rightarrow j}, \quad (6)$$

where $J_{i \rightarrow j} = p_i k_{i \rightarrow j} - p_j k_{j \rightarrow i}$ denotes the probability current with the transition rates,

$$k_{i \rightarrow j} = | \langle \epsilon_i | \hat{A} | \epsilon_j \rangle |^2 \Gamma(\omega_{ij}; \alpha_i), \quad (7)$$

where $\omega_{ij} = \epsilon_i - \epsilon_j$. The steady-state populations satisfy $\dot{p}_i = \sum_j J_{i \rightarrow j} = 0$. Note that the steady-state does not, in general, require the individual currents $J_{i \rightarrow j}$ to be zero. If, for every closed sequence of allowed transitions between energy levels $\epsilon_{i_1} \rightarrow \epsilon_{i_2} \rightarrow \dots \rightarrow \epsilon_{i_n} \rightarrow \epsilon_{i_1}$ with nonvanishing rates, Kolmogorov's loop condition, [36],

$$\sum_{r=1}^n \ln \frac{k_{i_r \rightarrow i_{r+1}}}{k_{i_{r+1} \rightarrow i_r}} = 0, \quad i_{n+1} \equiv i_1, \quad (8)$$

is satisfied then the steady-state populations obey a generalized detailed-balance relation,

$$\frac{p_j}{p_i} = \frac{k_{i \rightarrow j}}{k_{j \rightarrow i}} = e^{\beta_{\text{eff}}(\omega_{ij}; \alpha_i) \omega_{ij}},$$

and, equivalently, all individual probability currents vanish. In this case the stationary state assumes an exponential form,

$$\hat{\rho}^{\text{ss}} = \frac{1}{\sum_i e^{-F_i}} \sum_i e^{-F_i} |\epsilon_i\rangle \langle \epsilon_i|, \quad (9)$$

where F_i are obtained by fixing an arbitrary reference level i_0 and setting $F_{i_0} = 0$ and for any other level j , choosing an arbitrary sequence of allowed transitions connecting i_0 to j with non-zero rates $i_0 = i_1 \rightarrow i_2 \rightarrow \dots \rightarrow i_n = j$ and defining,

$$F_j = - \sum_{r=1}^{n-1} \ln \frac{k_{i_r \rightarrow i_{r+1}}}{k_{i_{r+1} \rightarrow i_r}}. \quad (10)$$

Interestingly, the above steady-state is not in the Gibbs form and Gibbs thermal state with unique temperature emerges only if the effective inverse temperatures become frequency independent, i.e. $\beta^{\text{eff}}(\omega; \alpha_i) = \beta$. In the absence of relative motion between the system and bath (i.e. $u = 0$), the standard detailed-balance condition $p_i/p_j = k_{ji}/k_{ij} = e^{\beta \omega_{ij}}$ recovered, implying that the steady-state reduces to Gibbs state of the form $\hat{\rho}^\beta = \frac{e^{-\beta \hat{H}_S}}{\text{Tr} e^{-\beta \hat{H}_S}}$. A two-level system which has only a single Bohr frequency ω is a trivial case for which the stationary state can always be written in the Gibbs form with a unique $\beta^{\text{eff}}(\omega) > 0$. However, it is not the case in general for multilevel systems with distinct transition frequencies ω_{ij} .

If the loop condition Eq. (8) is violated for at least one allowed closed cycle of transitions, then the system relaxes to a genuine NESS with persistent probability currents. In this case, no closed-form expression of the form Eq. (9) exists, and the steady-state must instead be obtained by solving $\dot{p}_i = - \sum_j J_{i \rightarrow j} = 0$. Note that while checking the loop condition Eq. (8), situations may arise where no closed sequence of allowed transitions exists due to the vanishing of certain matrix elements of the system operator entering the rates Eq. (7). This may occur, for instance, when certain transitions are forbidden

by symmetry of the system or by the specific form of system-bath coupling. In such cases when no allowed closed cycle of transitions is possible, probability currents are necessarily absent. The steady-state then still admits the exponential form Eq (9).

To see this explicitly, let us take the particular case of three-level system with interaction of the form,

$$\hat{A}^I(\tau) = \sum_{(ij) \in \{10, 21, 20\}} \lambda_{ij} (\hat{S}_{ij} e^{-i\omega_{ij}\tau} + \hat{S}_{ij}^\dagger e^{i\omega_{ij}\tau}), \quad (11)$$

where we define the lowering and raising operators,

$$\hat{S}_{10} = |\epsilon_1\rangle \langle \epsilon_0|, \quad \hat{S}_{21} = |\epsilon_2\rangle \langle \epsilon_1|, \quad \hat{S}_{20} = |\epsilon_2\rangle \langle \epsilon_0|, \quad (12)$$

satisfying $[H_S, S_{ij}] = -\omega_{ij} S_{ij}$ with Bohr frequencies $\omega_{ij} = \epsilon_i - \epsilon_j > 0$ and $S_{ji} = S_{ij}^\dagger$. Note that we assume non-degenerate and well-separated Bohr frequencies such that the secular approximation is valid. We define the cycle affinity,

$$\begin{aligned} \mathcal{A} &= \ln \frac{k_{2 \rightarrow 0} k_{0 \rightarrow 1} k_{1 \rightarrow 2}}{k_{0 \rightarrow 2} k_{1 \rightarrow 0} k_{2 \rightarrow 1}} \\ &= \beta_{\text{eff}}(\omega_{20}; \beta, u) \omega_{20} - \beta_{\text{eff}}(\omega_{21}; \beta, u) \omega_{21} \\ &\quad - \beta_{\text{eff}}(\omega_{10}; \beta, u) \omega_{10}. \end{aligned} \quad (13)$$

For $u = 0$, $\beta_{\text{eff}}(\omega; \beta, u) \equiv \beta$, implying $\mathcal{A} = 0$. For $u \neq 0$, one generically finds $\mathcal{A} \neq 0$ and a nonzero steady-state probability current. For three-level system, the steady-state currents along each transition are equal (see [35]),

$$\mathcal{J} \equiv J_{0 \rightarrow 1}^{\text{ss}} = J_{1 \rightarrow 2}^{\text{ss}} = J_{2 \rightarrow 0}^{\text{ss}}. \quad (14)$$

In addition, to maintain the system in NESS, we also have a non-zero entropy production rate $\Sigma = \mathcal{J} \mathcal{A} \geq 0$. We adopt the convention that $\mathcal{J} > 0$ denotes current along $0 \rightarrow 1 \rightarrow 2 \rightarrow 0$. Also the sign(\mathcal{J}) = sign(\mathcal{A}). In the small-velocity limit $u \ll 1$,

$$\beta_{\text{eff}}(\omega; \beta, u) \approx \beta \left[1 + \frac{u^2}{2} - \frac{u^2}{6} \beta \omega \coth\left(\frac{\beta \omega}{2}\right) \right], \quad (15)$$

and using $\omega_{20} = \omega_{21} + \omega_{10}$ one finds,

$$\begin{aligned} \mathcal{A} &\approx \frac{\beta^2 u^2}{6} \left[\omega_{10}^2 \coth\left(\frac{\omega_{10}\beta}{2}\right) + \omega_{21}^2 \coth\left(\frac{\omega_{21}\beta}{2}\right) \right. \\ &\quad \left. - (\omega_{10} + \omega_{21})^2 \coth\left(\frac{(\omega_{10} + \omega_{21})\beta}{2}\right) \right]. \end{aligned} \quad (16)$$

Moreover, using the inequality,

$$(a+b)^2 \coth\left(\frac{(a+b)\beta}{2}\right) \geq a^2 \coth\left(\frac{a\beta}{2}\right) + b^2 \coth\left(\frac{b\beta}{2}\right), \quad (17)$$

for $a, b \geq 0$, we see that $\mathcal{A} \leq 0$ to order u^2 . Therefore, for small u the current circulates opposite to the chosen convention with $\mathcal{J} < 0$ (i.e. the current flows along $0 \rightarrow 2 \rightarrow 1 \rightarrow 0$).

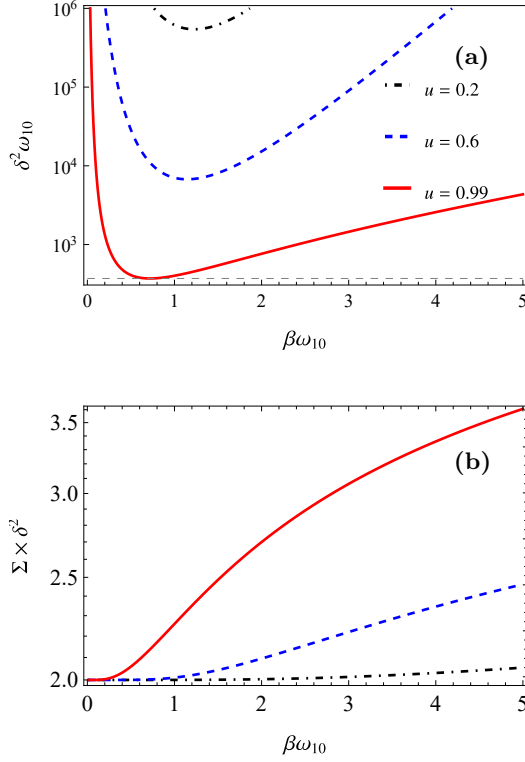


FIG. 2. (Color Online) Relative uncertainty δ^2 (a) and product of relative uncertainty with entropy production $\delta^2 \Sigma$ (b) as a function of inverse temperature β for different values of velocity u . Other parameter values are same as Fig. (1).

Fig. 1 shows that relativistic motion induces a NESS characterized by a nonzero affinity and probability current. More specifically, Fig. 1(a) displays the affinity \mathcal{A} as a function of the bath rest frame inverse temperature β for different system velocities u . The affinity vanishes as $u \rightarrow 0$ and becomes increasingly negative as u increases, reaching its largest magnitude in the low-temperature and ultrarelativistic regime. The negative sign reflects the direction of the steady-state current, consistent with the sign predicted in the small-velocity limit discussed above, and persists even beyond that. Fig. 1(b) shows the corresponding steady-state current \mathcal{J} . Its magnitude increases from zero at high temperatures ($\beta \rightarrow 0$), attains a maximum at an intermediate inverse temperature, and decays again in the low-temperature limit ($\beta \rightarrow \infty$). We find that in the weak-driving regime $\mathcal{A} \ll 1$, the current is approximately linear, $\mathcal{J} \approx K_0 \mathcal{A}$, where K_0 depends only on β and the Bohr frequencies ω_{10} and ω_{21} . Since $\mathcal{A} \propto u^2$ for $u \ll 1$, this implies $\mathcal{J} \propto u^2$ at low velocities. While \mathcal{A} increases with β , the coefficient K_0 decreases, their competition yields an optimal β of order of the system's Bohr frequencies.

Stochastic clock— Here we show that the three-level system NESS with persistent current can be a model of stochastic clock [37, 38]. We count the net transition from

$2 \rightarrow 0$ and call it one cycle, and define one tick as one complete cycle (see [35]). The stochastic variable $n(\tau)$ keeps count of the transitions such that for $2 \rightarrow 0$ the variable increases by +1 and for $0 \rightarrow 2$ decreases by -1. In the long time limit we have,

$$\langle n \rangle_\tau \approx \mathcal{J} \tau, \quad \text{Var}(n)_\tau \approx 2D\tau, \quad (18)$$

where \mathcal{J} is steady-state current defined before and D is the diffusion constant. For the performance of the stochastic clock, we look at two quantities,

$$\mathcal{J} = \frac{\langle n \rangle_\tau}{\tau}, \quad \delta^2 = \frac{2D}{\mathcal{J}^2}, \quad (19)$$

where steady-state current \mathcal{J} be interpreted as number of cycles per unit time and δ^2 characterizes relative uncertainty per unit time. In time interval τ , we expect to read $\mathcal{J}\tau$ number of cycles on average with relative uncertainty $\delta \frac{1}{\sqrt{\tau}}$.

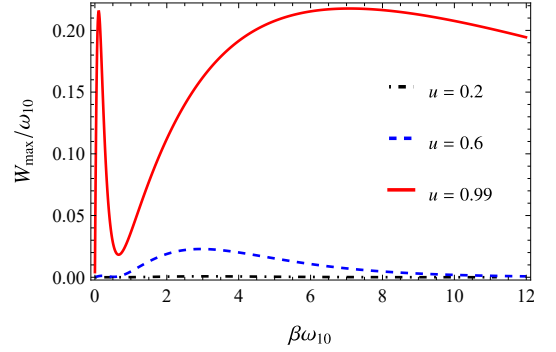


FIG. 3. (Color Online) Plot of maximum extractable work W_{\max} of steady-state $\hat{\rho}^{\text{ss}}$ for different values of velocity u . Other parameter values are same as Fig. (1)

Fig. (2) shows the relative uncertainty and entropy production for the stochastic clock. Specifically, Fig. 2(a) displays the relative uncertainty δ^2 as a function of the bath rest frame inverse temperature β for different velocities u . Similar to the behavior of the current, δ^2 exhibits a minimum at an intermediate value of β , with a minimum uncertainty of order $\delta^2 \sim 10^2 \omega_{10}^{-1}$, indicating that fluctuations remain significantly high. The energetic cost of maintaining the NESS is quantified by the entropy production rate $\Sigma = \mathcal{J}\mathcal{A}$, which is constrained by the thermodynamic uncertainty relation (TUR),

$$\delta^2 \Sigma \geq 2. \quad (20)$$

Fig. 2(b) shows the product $\delta^2 \Sigma$, which remains well above the bound and approaches it only close to equilibrium, where $u \rightarrow 0$ and $\mathcal{A} \rightarrow 0$. This reflects the usual dissipation-precision tradeoff and shows that the system does not efficiently convert entropy production into improved precision. We conclude that overall, the

model acts as a stochastic clock with a finite ticking rate, but the large relative uncertainty implies strong noise. However, over long observation times, the error decreases as $1/\sqrt{\tau}$, indicating that the system should, in principle, still provide a reliable elapsed time.

Quantum battery— In the interaction Eq. (11), we set $\lambda_{01} = 0$, so only $2 \leftrightarrow 0$ and $2 \leftrightarrow 1$ transitions are allowed and $1 \leftrightarrow 0$ is forbidden then for steady-state each current individually vanishes i.e. $J_{2 \rightarrow 0}^{\text{ss}} = J_{1 \rightarrow 2}^{\text{ss}} = 0$, and the steady-state in the exponential form reads,

$$\hat{\rho}^{\text{ss}} = p_0^{\text{ss}} |\epsilon_0\rangle \langle \epsilon_0| + p_1^{\text{ss}} |\epsilon_1\rangle \langle \epsilon_1| + p_2^{\text{ss}} |\epsilon_2\rangle \langle \epsilon_2|, \quad (21)$$

where,

$$p_0^{\text{ss}} = \frac{1}{A_0}, p_1^{\text{ss}} = \frac{e^{\beta_{\text{eff}}(\omega_{21})\omega_{21} - \beta_{\text{eff}}(\omega_{20})\omega_{20}}}{A_0}, p_2^{\text{ss}} = \frac{e^{-\beta_{\text{eff}}(\omega_{20})\omega_{20}}}{A_0}, \quad (22)$$

with normalisation,

$$A_0 = 1 + e^{\beta_{\text{eff}}(\omega_{21})\omega_{21} - \beta_{\text{eff}}(\omega_{20})\omega_{20}} + e^{-\beta_{\text{eff}}(\omega_{20})\omega_{20}}. \quad (23)$$

Although there is no persistent current, we show that it still exhibits finite non-equilibrium free energy that can be used for work storage or extraction. First, we show that the steady-state has vanishing ergotropy. Note that since there is no coherence in the steady-state, we need to have population inversion, i.e. $p_i^{\text{ss}} > p_j^{\text{ss}}$ for $\epsilon_i > \epsilon_j$ to get non-zero ergotropy. By looking at the expression for the ratios of probabilities, we can see that since $\beta_{\text{eff}}(\omega) > 0$, we always have $p_2^{\text{ss}} < p_0^{\text{ss}}$ and $p_2^{\text{ss}} < p_1^{\text{ss}}$. So to get population inversion, we should have $p_1^{\text{ss}} > p_0^{\text{ss}}$. This is true only if we have,

$$\omega_{21}\beta_{\text{eff}}(\omega_{21}) - \omega_{20}\beta_{\text{eff}}(\omega_{20}) > 0. \quad (24)$$

However this condition never satisfied given that $N(\omega, \beta, u)$ is strictly decreasing function of ω and,

$$\begin{aligned} \ln \frac{N(\omega_{21}, \beta, u) + 1}{N(\omega_{21}, \beta, u)} &< \ln \frac{N(\omega_{20}, \beta, u) + 1}{N(\omega_{20}, \beta, u)} \\ \implies \omega_{21}\beta_{\text{eff}}(\omega_{21}) - \omega_{20}\beta_{\text{eff}}(\omega_{20}) &< 0. \end{aligned} \quad (25)$$

This implies no population inversion either and the ergotropy of the steady-state must be zero. Although this means one cannot extract any work using a cyclic unitary process from this state, one can still extract the work if interaction with a bath is allowed [39] or many identical copies of the system are available [40] since the steady-state is not the Gibbs thermal state. The maximum extractable work is quantified by the non-equilibrium free energy difference between the given steady-state and the reference Gibbs thermal state.

$$\mathcal{W}_{\text{max}} = \mathcal{F}(\hat{\rho}^{\text{ss}}) - \mathcal{F}(\hat{\rho}^\beta) = \frac{1}{\beta} D(\hat{\rho}^{\text{ss}} || \hat{\rho}^\beta), \quad (26)$$

where $\mathcal{F}(\hat{\rho}) = \text{Tr}(\hat{H}_S \hat{\rho}) - \frac{1}{\beta} S(\hat{\rho})$, $S(\hat{\rho}) = -\text{Tr}[\hat{\rho} \ln \hat{\rho}]$ is von Neumann entropy, $\hat{\rho}^\beta = \frac{e^{-\beta \hat{H}_S}}{\text{Tr} e^{-\beta \hat{H}_S}}$ is reference Gibbs thermal state at bath temperature in its rest frame β , and $D(\hat{\rho} || \hat{\sigma}) = \text{Tr}[\hat{\rho}(\ln \hat{\sigma} - \ln \hat{\rho})]$ is quantum relative entropy. We define the reference temperature as the bath rest frame temperature β . Although one might attempt to define a temperature in the systems comoving frame, no unique inverse temperature can be assigned to a relativistically moving bath [29]. Now substituting (21) in to (26) and simplifying we get,

$$\begin{aligned} \beta \mathcal{W}_{\text{max}} &= p_0^{\text{ss}} \omega_{20} [\beta_{\text{eff}}(\omega_{20}) - \beta] + p_1^{\text{ss}} \omega_{21} [\beta_{\text{eff}}(\omega_{21}) - \beta] \\ &\quad + \log \frac{Z_\beta}{A_0}. \end{aligned} \quad (27)$$

Fig. 3 shows the maximum extractable work \mathcal{W}_{max} as a function of the bath rest-frame inverse temperature β for different velocities u . We observe that \mathcal{W}_{max} vanishes in both the high-temperature ($\beta \rightarrow 0$) and low-temperature ($\beta \rightarrow \infty$) limits, while exhibiting a pronounced peak followed by a broad maximum at intermediate values of β . This non-monotonic behavior originates from the deviation between the effective inverse temperature $\beta_{\text{eff}}(\omega; \beta, u)$ corresponding to the largest energy gap of three level system and the bath rest frame inverse temperature β . In the high-temperature regime, $\beta \rightarrow 0$, the steady state approaches a maximally mixed state, rendering work extraction impossible. As the temperature is lowered (increasing β), $\beta_{\text{eff}}(\omega; \beta, u)$ becomes larger than β , and the growing difference produces the first peak in \mathcal{W}_{max} . With further increase of β , $\beta_{\text{eff}}(\omega; \beta, u)$ crosses the bath rest frame inverse temperature value, $\beta_{\text{eff}} = \beta$, suppressing work extraction and producing the dip observed in Fig. 3. Beyond this point, $\beta_{\text{eff}}(\omega; \beta, u) < \beta$, and enables work extraction, giving rise to the broad maximum at larger β . Finally, in the low-temperature limit $\beta \rightarrow \infty$, both β and $\beta_{\text{eff}}(\omega; \beta, u)$ diverge, the steady state approaches the ground state, and \mathcal{W}_{max} vanishes.

Discussion—To show NESS with non-zero affinity, we have considered the Δ configuration of a three-level system. In nature, most three-level systems coupling to the EM field appear in the Λ , V , or Ξ configurations, with one of the transitions forbidden due to symmetry and dipole selection rules. Nonetheless, such configurations can occur in certain chiral molecules, where the lack of symmetry permits all dipole matrix elements to be nonzero [41]. Moreover, artificial atoms (for example, in superconducting circuits) are not limited by symmetry constraints and provide a controllable platform to engineer Δ -type systems [42].

Also, to maintain NESS with non-zero current, the system continuously consumes non-equilibrium resources and dissipates heat. The resource here is actually coming from the energy spent in maintaining the relative motion of the system and bath. This also implies that there must be some drag force experienced by the system moving

through the bath, allowing it to dissipate the heat. This is in agreement with the studies on drag force called Einstein–Hopf drag/ quantum friction experienced by moving quantum systems in blackbody radiation [43]. Note, however, in the case of a quantum battery, we have $\mathcal{A} = 0$, and there is no entropy production required to maintain the non-Gibbs steady-state. There, the extractable work must have been injected during the transient dynamics responsible for driving the system away from the Gibbs state.

Conclusion—In this work, we have considered a localized quantum system moving at uniform relativistic velocity through a thermal bath consisting of a massless scalar field. We showed that relative motion alone is sufficient to drive the system into a NESS, even in the presence of a single thermal bath. The underlying physical mechanism is the modification of the KMS condition followed by bath correlation function evaluated on the trajectory of the system, which lead to generalized detailed balance relation for the system and prevents relaxation to a Gibbs state. We found that the steady states fall into two classes: NESS with persistent probability current and current-free non-Gibbs steady states in exponential form. Focusing on a three-level system, we demonstrated that a NESS with persistent probability current may operate as a noisy stochastic clock, while a current-free non-Gibbs state possesses finite non-equilibrium free energy and can function as a quantum battery. These findings place relativistic motion alongside other thermodynamical resources like coherence, squeezing, multiple baths, etc.

Finally, several extensions of the work are possible. Although we have shown that uniform relativistic motion generically leads to a non-Gibbs steady state, the absence of population inversion and vanishing ergotropy suggests that this setup does not realize maximal thermodynamic advantage. A natural next step is therefore to explore other stationary trajectories and determine whether stronger thermodynamic resources can emerge in different setups. Another important direction is to consider systems moving in curved spacetime rather than flat spacetime considered here, for example in the vicinity of black holes, where spacetime geometry itself may influence steady-state properties and potentially enable new forms of thermodynamic resource. Finally, while our study focuses on a localized system interacting with a scalar field, it would be interesting to extend the analysis to EM field [44], spatially extended systems, and multiple systems where collective effects may further enrich the steady-state behavior.

Acknowledgements.—The author thanks B. P. Venkatesh, K. Adhikary, and V. Singh for useful comments.

-
- * rahulkumarkishorbhai.shastri@upol.cz
- [1] M. O. Scully, M. S. Zubairy, G. S. Agarwal, and H. Walther, *Science* **299**, 862 (2003).
 - [2] R. Dillenschneider and E. Lutz, *Europhys. Lett.* **88**, 50003 (2009).
 - [3] J. Roßnagel, O. Abah, F. Schmidt-Kaler, K. Singer, and E. Lutz, *Phys. Rev. Lett.* **112**, 030602 (2014).
 - [4] J. Klaers, S. Faelt, A. Imamoglu, and E. Togan, *Phys. Rev. X* **7**, 031044 (2017).
 - [5] W. Niedenzu, V. Mukherjee, A. Ghosh, A. G. Kofman, and G. Kurizki, *Nat. Commun.* **9**, 165 (2018).
 - [6] R. Uzdin, A. Levy, and R. Kosloff, *Phys. Rev. X* **5**, 031044 (2015).
 - [7] S. Bhattacharjee and A. Dutta, *Eur. Phys. J. B* **94**, 239 (2021).
 - [8] F. Campaioli, S. Gherardini, J. Q. Quach, M. Polini, and G. M. Andolina, *Rev. Mod. Phys.* **96**, 031001 (2024).
 - [9] M. T. Mitchison, *Contemp. Phys.* **60**, 164 (2019).
 - [10] A. Pozas-Kerstjens and E. Martín-Martínez, *Phys. Rev. D* **92**, 064042 (2015).
 - [11] H. Nystrom, N. Pranzini, and E. Keski-Vakkuri, *Phys. Rev. Res.* **7**, 033085 (2025).
 - [12] E. Arias, T. R. de Oliveira, and M. S. Sarandy, *J. High Energy Phys.* **2018** (2), 168.
 - [13] N. Papadatos, *Int. J. Theor. Phys.* **60**, 4210 (2021).
 - [14] D. Barman and B. R. Majhi, *J. High Energy Phys.* **2022** (5), 46.
 - [15] E. E. Ferketec and S. Deffner, *Europhys. Lett.* **141**, 19001 (2023).
 - [16] K. Gallock-Yoshimura, V. Thakur, and R. B. Mann, *Front. Phys.* **11**, 10.3389/fphy.2023.1287860 (2023).
 - [17] V. Shaghghi, P. Chattopadhyay, V. V. Nautiyal, K. Chatterjee, T. Pandit, and V. Singh, *arXiv:2508.20692*.
 - [18] D. Moustos and O. Abah, *arXiv:2508.11554*.
 - [19] T. Hirofani and K. Gallock-Yoshimura, *Phys. Rev. D* **111**, 125023 (2025).
 - [20] A. Mukherjee, S. Gangopadhyay, and A. S. Majumdar, *arXiv:2411.02849*.
 - [21] Y. Chen, W. Zhang, T. Ren, and X. Hao, *arXiv:2503.02472*.
 - [22] M. Ahmadi, D. E. Bruschi, and I. Fuentes, *Phys. Rev. D* **89**, 065028 (2014).
 - [23] Z. Tian, J. Wang, H. Fan, and J. Jing, *Sci. Rep.* **5**, 7946 (2015).
 - [24] S. Robles and J. Rodríguez-Laguna, *J. Stat. Mech.* **2017**, 033105 (2017).
 - [25] X. Liu, J. Jing, Z. Tian, and W. Yao, *Phys. Rev. D* **103**, 125025 (2021).
 - [26] H. Rangani Jahromi, S. Ebrahimi Asl Mamaghani, and R. Lo Franco, *Ann. Phys.* **448**, 169172 (2023).
 - [27] S. S. Costa and G. E. A. Matsas, *Phys. Rev. D* **52**, 3466 (1995).
 - [28] L. Accardi and K. Imafuku, *arXiv:quant-ph/0209088*.
 - [29] N. Papadatos and C. Anastopoulos, *Phys. Rev. D* **102**, 085005 (2020).
 - [30] M. Good, B. A. Juárez-Aubry, D. Moustos, and M. Temirkhan, *Journal of High Energy Physics* **2020**, 59 (2020).
 - [31] T. R. Perche, *Phys. Rev. D* **104**, 065001 (2021).
 - [32] C. R. D. Bunney, L. Parry, T. R. Perche, and J. Louko, *Phys. Rev. D* **109**, 065001 (2024).

- [33] A. G. Pasetegger and R. Verch, [Rev. Math. Phys. **37**, 2430009 \(2025\)](#).
- [34] J. R. Letaw, [Phys. Rev. D **23**, 1709 \(1981\)](#).
- [35] See supplementary material for additional details.
- [36] J. Schnakenberg, [Rev. Mod. Phys. **48**, 571 \(1976\)](#).
- [37] A. C. Barato and U. Seifert, [Phys. Rev. X **6**, 041053 \(2016\)](#).
- [38] P. Erker, M. T. Mitchison, R. Silva, M. P. Woods, N. Brunner, and M. Huber, [Phys. Rev. X **7**, 031022 \(2017\)](#).
- [39] G. Manzano, F. Plastina, and R. Zambrini, [Phys. Rev. Lett. **121**, 120602 \(2018\)](#).
- [40] R. Alicki and M. Fannes, [Phys. Rev. E **87**, 042123 \(2013\)](#).
- [41] Chong Ye, Quansheng Zhang, and Yong Li, [Phys. Rev. A **98**, 063401 \(2018\)](#).
- [42] Y. Liu, J. You, L. Wei, C. Sun, and F. Nori, [Phys. Rev. Lett. **95**, 087001 \(2005\)](#).
- [43] G. Lach, M. DeKieviet, and U. D. Jentschura, [Phys. Rev. Lett. **108**, 043005 \(2012\)](#).
- [44] Huabing Cai and Li-Gang Wang, [Phys. Lett. A **440**, 128148 \(2022\)](#).